Asian Journal of Chemistry; Vol. 28, No. 7 (2016), 1453-1462

ASIAN JOURNAL OF CHEMISTRY

http://dx.doi.org/10.14233/ajchem.2016.19686

Corrosion Resistance of AA2036 and AA7075-T651 in Contaminated Acid Chloride Environments

M. ABDULWAHAB[1,2], A.P.I. POPOOLA[1,*], O.E. OLADIJO[1], C.O. LOTO[1,3] and O.P. OLADIJO[4]

[1]Department of Chemical, Metallurgical and Materials Engineering, Tshwane University of Technology, Pretoria, South Africa
[2]Department of Metallurgical and Materials Engineering, Ahmadu Bello University, Zaria, Nigeria
[3]Department of Mechanical Engineering, Covenant University, Ota, Nigeria
[4]Department of Mechanical Engineering, Botswana International University of Technology, Palapye, Botswana

*Corresponding author: E-mail: popoolaapi@tut.ac.za

Received: 22 October 2015; *Accepted*: 4 February 2016; *Published online*: 31 March 2016; AJC-17829

In the present study, an assessment on corrosion resistance of aluminium alloys type AA2036 and AA7075-T651 in varying solution consisting of acidic, saline and in contaminated acid-chloride environments was investigated using weight loss and electrochemical techniques. The as-received samples were sectioned into corrosion coupons polished, degreased and weight taken. Solutions containing 3.5 % NaCl, 0.5 M HCl, 0.5 M H_2SO_4 were prepared as corrosion media and combination of these solutions were used as contaminated environment for the samples. In the weight loss method, the samples were exposed separately in each solution and it combinations for period of 3 to 60 days (72 to 1440 h). While in the electrochemical method, a potentiostat corrosion kit was used. The scanning electron microscope and X-ray diffractometry were used to characterize the as-corroded samples. The corrosion rate of the alloy decreases with increase in exposure time. The corrosion rate of AA2036 in NaCl solution was observed to be the lowest (0.058253 mm/yr) as compare with AA7075-T651 (0.14273 mm/yr) in the same environmental conditions indicating a 59 % improvement. From the SEM surface morphology, the evidence of pitting corrosion attack was found when the samples are used in a various contaminated acid-chloride environments. The XRD spectra of the samples immersed in contaminated 0.5 M H_2SO_4 with NaCl for AA2xxx and AA7xxx comprised of Al (FCC structure), while H_2SO_4 (H_2O) with an unknown peak found at $2\theta = 82°$ detected on the corroded AA7xxx series. It was observed that the corrosion potentials of the alloy were practically reduced when in any of the contaminated environments.

Keywords: AA2036, AA7075, Contaminated solution, Corrosion potentials, Active-passive, Interfaces, Phases.

INTRODUCTION

Aluminium alloys have been the primary material of choice for structural components of aircraft over the years [1]. Although some polymer matrix composites are being used extensively in high-performance military aircrafts and are specified for some applications in modern commercial aircraft. However, aluminium alloys are the overwhelming choice for the wing, military cargo and transport. The uniqueness characteristic, fabrication costs, design experiment are some of the reason for the continued confidence in aluminium alloys that will ensure their use in significant qualities for the rest of this century [2]. A unique combination of properties makes aluminium and its alloy one of the most versatile engineering and construction materials available today such as light weight, excellent corrosion, strong low temperature, easy to work, good heat conductor, high reflectivity, good electrical conductor, non-magnetic *etc*. [3-7]. These are characteristics that gave aluminium its extreme wide application. In the majority of applications, two or more of these characteristic come prominently into play; for example, light weight combined with strength in aircraft, railway rolling stock, trucks and other transportation equipment. High resistance and high thermal conductivity are important for chemical and petroleum industries. High reflectivity, excellent weathering characteristics and light weight are all important in roofing material.

Aluminium and its alloys are generally passive and corrosion resistant in aqueous solutions except for pitting corrosion due to some reactive species, such as chloride [8]. Aluminium has a natural corrosion protection from its oxide layer, but if exposed to aggressive environments it may corrode. From a purely thermodynamically point of view aluminium is active. However, in oxygen containing environment (air, water), aluminium is rapidly covered with a dense oxide layer [9]. Although in varying number of service conditions, such as in contaminated and highly aggressive environment, the alloy may surfer several corrosive attacks. In the present study the corrosion resistance of aluminium alloys type AA2036 and

AA7075-T651 in separate and contaminated-acid-chloride environments was studied with detailed surface and X-ray diffraction analysis using the weight loss and potentiodynamic polarization techniques.

EXPERIMENTAL

The substrate material used for the study are AA2023 and AA7075-T651 obtained from metal alloys company in Pretoria. These materials were used for these studies based on their extensive application in the petrochemical and aircraft industries. The chemical compositions of the as-received substrates are shown in Tables 1 and 2.

Corrosion media and preparation: The corrosion media used are 3.5 % wt sodium chloride, 0.5 M sulphuric acid, 0.5 M hydrochloride acid and a contaminated solution containing H_2SO_4 with NaCl/HCl with NaCl solution. Equally, 0.5 M sulphuric acid with 3.5 % sodium chloride and 0.5 M hydrochloric acid solutions with 3.5 % sodium chloride were prepared from an analytical grade H_2SO_4 (98 %) and HCl (37 %) with appropriate dilution of distilled water and was used as corrosive media for this study.

Weight loss and linear polarization method: For weight loss experiment, the cleaned and weighed coupons with drilled hole at one end of each coupons measured 3 mm diameter were fully immersed with aid of inelastic thread and rod in 200 mL of each of the corrosive media. At every 72 h the coupons was taken out of the test media, thoroughly washed with distilled water, rinsed with acetone, dried and re-weighed again. The experiment was conducted for 1440 h. The weight loss and corrosion rate were determined.

Linear polarization measurements were carried out in a three-electrode corrosion cell. A silver chloride electrode (Ag/AgCl) containing 3 M/L of KCl was used as reference electrode, a graphite rod was used as counter electrode while aluminium alloy as working electrode. The polarization studies were conducted at room temperature in 3.5 % wt NaCl, 0.5 M H_2SO_4, 0.5 M HCl, 0.5 M H_2SO_4 with 3.5 % wt NaCl and 0.5 M HCl with 3.5 % wt NaCl using AUTOLAB Potentiostat (model Reference-668), which was connected to an acquisition system to control the experiments and NOVA software packaged with version 1.8 was used in analyzing the data. The measurements were made from -1.5V to +1.5V at scan rate of 0.00016 v/sec from the Tafel analysis; corrosion current density, corrosion rate, linear polarization resistance and corrosion potential were obtained.

X-ray diffraction (XRD) analysis and scanning electron microscopy (SEM): A Philips PW 1713 X-ray diffractometer fitted with a monochromatic CuK_α radiation set at 40 kV and 20 mA was used to determine the phase composition of the as-received substrates as well as as-corroded surfaces. The scan was taken between 10° and 80° 2θ with a step size of 0.02°. Phase and compound identification was performed using Philips Analytical X'Pert High Score® software with an in-built International Centre for Diffraction Data (ICSD) database.

For microstructural analysis, as-received substrate sample were prepared by cutting into squares of 1.5 cm and were mounted in bakelite (hot mounted), in a chuck device, where they could be polished using sequentially metallographic finer grades of SiC abrasive paper: 120, 320, 400, 600 1000 to 1200 grade. They were then polished with a cloth sequentially using diamond paste of 6, 3 and 1 µm to obtain a mirror-like surface. The surface was then rinsed in distilled water and degreased with acetone, dried and stores in a dessicator which were later etched. However, for as-corroded samples, the microstructures were identified immediately from corrosion study with above procedures for surface degradation investigation.

RESULTS AND DISCUSSION

Influence of exposure time on the corrosion rate and polarization resistance of AA2036 and AA7075-T651 in acid/saline-contaminated environments: The corrosion resistance of the AA2036 and AA7075-T651 in NaCl solution increased with exposure time (Fig. 1). In Fig. 1, AA7075-T651 has better corrosion resistance than AA2036 when immersed in NaCl solution. However in Fig. 2, the two aluminium alloys have an increased corrosion rate with exposure time. Although in the H_2SO_4 solution there seems to be lower corrosion rate for AA2036 alloy. While in HCl solution, the corrosion rate for the aluminium alloys decreased drastically along with exposure time indicating a lower corrosion rate in AA7075-

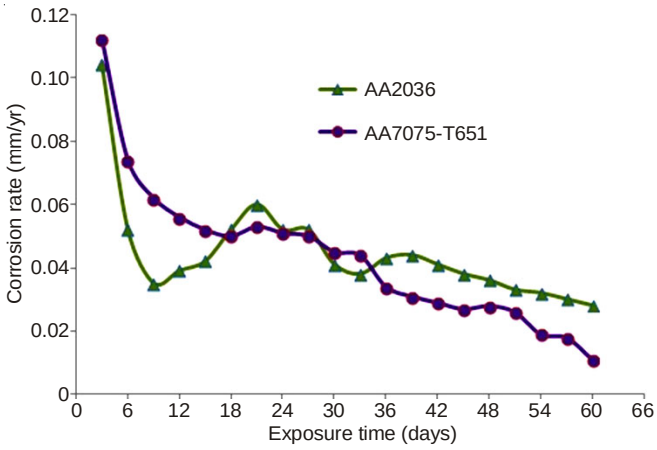

Fig. 1. Corrosion rate of AA2036 and AA7075-T651 in 3.5 % NaCl

TABLE-1
CHEMICAL COMPOSITION OF AA2036 (% wt)

Element	Si	Fe	Cu	Mn	Mg	Cr	Ti	Ca	Zn	V	Al
wt %	0.0302	0.0559	2.40	0.289	0.673	0.0260	0.0262	0.0542	0.0217	0.007	Balance

TABLE-2
CHEMICAL COMPOSITION OF AA7075-T651 (% wt)

Element	Si	Fe	Cu	Mn	Mg	Cr	Ti	Ca	Zn	V	Al
wt %	0.157	0.282	0.0025	0.024	0.51	0.023	0.006	0.0011	0.002	0.0035	Balance

TABLE-3
LINEAR POLARIZATION MEASUREMENT OF AA2036 AND AA7075-T651 SUBSTRATES IN ACID, SALINE AND CONTAMINATED ENVIRONMENT

Samples	β_c (V/dec)	β_a (V/dec)	I_{corr} (A/cm^2)	i_{corr} (A)	LPR R_p (Ω)	$-E_{corr}$ (V)	Corrosion rate (mm/yr)
AA2036 in 3.5 % wt NaCl	0.08176	0.35012	5.06×10^{-6}	5.06×10^{-6}	5693.1	1.0089	0.058253
AA7075-T651 in 3.5 % wt NaCl	0.14813	0.35423	3.58×10^{-5}	2.90×10^{-5}	1564.1	1.1389	0.14273
AA2036 in 0.5 M H_2SO_4	0.21357	0.11166	2.47×10^{-5}	2.47×10^{-5}	1291.6	0.56751	0.27591
AA7075-T651 in 0.5 M H_2SO_4	0.75954	0.16444	2.69×10^{-5}	2.69×10^{-5}	2179	0.61428	0.41872
AA2036 in 0.5 M HCl	0.16234	0.05849	8.77×10^{-4}	6.32×10^{-4}	39.565	0.7678	9.816
AA7075-T651 in 0.5 M HCl	0.16567	0.11349	5.19×10^{-4}	5.19×10^{-4}	56.323	0.5848	6.9826
AA2036 in 0.5 M H_2SO_4 + 3.5 % wt NaCl	0.10507	0.14758	7.17×10^{-4}	8.61×10^{-4}	60.98	0.5721	8.2585
AA7075-T651 in 0.5 M H_2SO_4 + 3.5 % wt NaCl	0.24396	0.11754	9.79×10^{-4}	7.05×10^{-4}	48.884	0.76153	10.953
AA2036 in 0.5 M HCl+ 3.5 % wt NaCl	0.15446	0.11754	6.51×10^{-4}	7.81×10^{-4}	60.84	0.6175	11.446
AA7075-T651 in 0.5 M HCl+ 3.5 % wt NaCl	0.18683	0.25861	1.49×10^{-3}	1.08×10^{-3}	43.83	0.78854	16.706

T651 than AA2036 (Fig. 3). This agreed with the work of Hijazi *et al*. [6] and David [10]. Similar trend was observed for the contaminated H_2SO_4-chloride (Fig. 4) and HCl-chloride environment (Fig. 5). The corrosion resistance of the AA2036 can be said to be higher than that of AA7075-T651 throughout the exposure time considered.

This corresponds with the result obtained by potentiodynamic polarization method. In which the corrosion rate of AA2036 in NaCl is the lowest (0.058253 mm/yr) as compare with AA7075-T651 (0.14273 mm/yr) under the same experimental conditions (Table-3). This means it has higher corrosion

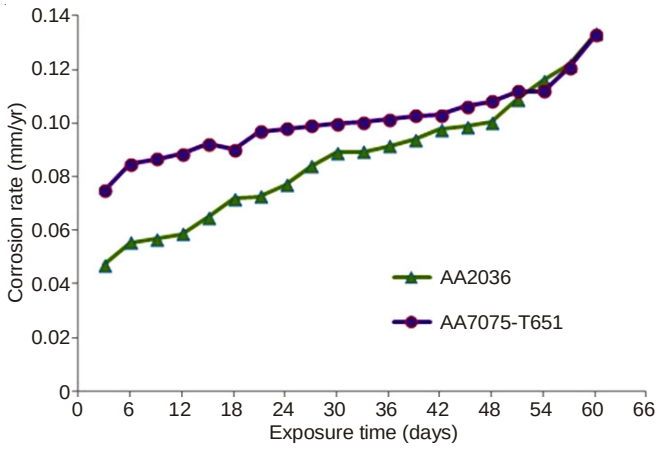

Fig. 2. Corrosion rate for AA2036 and AA7075-T651 in 0.5 M H_2SO_4

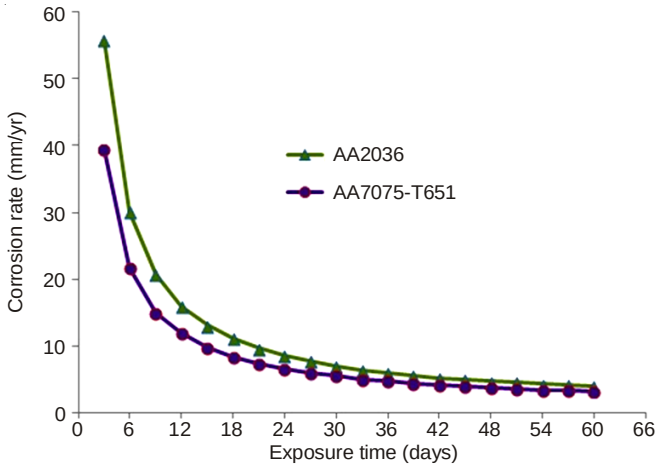

Fig. 3. Corrosion rate for AA2036 and AA7075-T651 in 0.5 M HCl

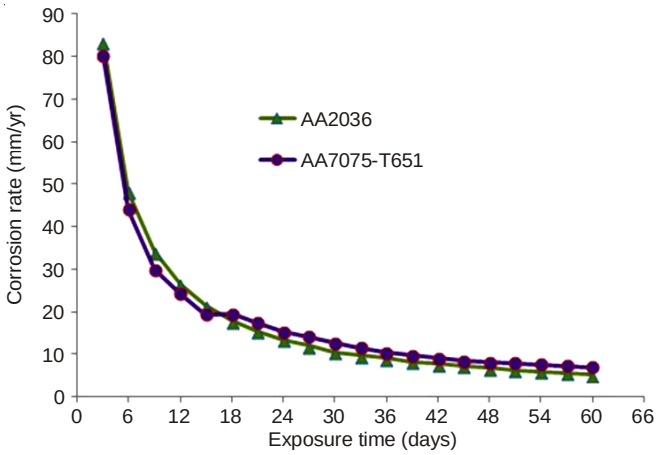

Fig. 4. Corrosion rate for AA2036 and AA7075-T651 in a contaminated 0.5 M H_2SO_4 with 3.5 % NaCl solution

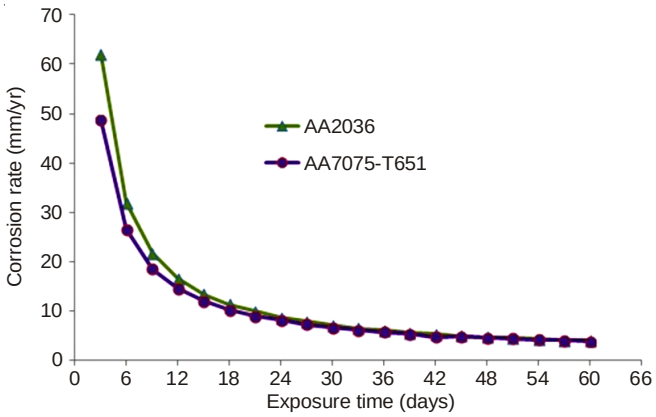

Fig. 5. Corrosion rate for AA2036 and AA7075-T651 in a contaminated 0.5 M HCl with 3.5 % NaCl solution

potential than AA7075-T651 (Fig. 6) indicating a 59 % (over 2 times) improvement. Similarly, in H_2SO_4 solution, AA2036 alloy still exhibits the lowest corrosion rate, indicating higher protection against corrosion attack (Fig. 7). But in HCl solution, the corrosion rate of AA2036 became higher than AA7075-T651 (Fig. 8) with polarization resistance of 39.565 and 56.323 Ω, respectively. In the contaminated acid-chloride solution, AA2036 alloy in H_2SO_4 with NaCl have the lowest corrosion rate (Figs. 9 and 10). In particular AA2036 (Fig. 9) have 8.2585 mm/yr and AA7075-T651 (Fig. 10) with 16.706 mm/yr indicating a half value reduction. This analysis means that AA2036 alloy

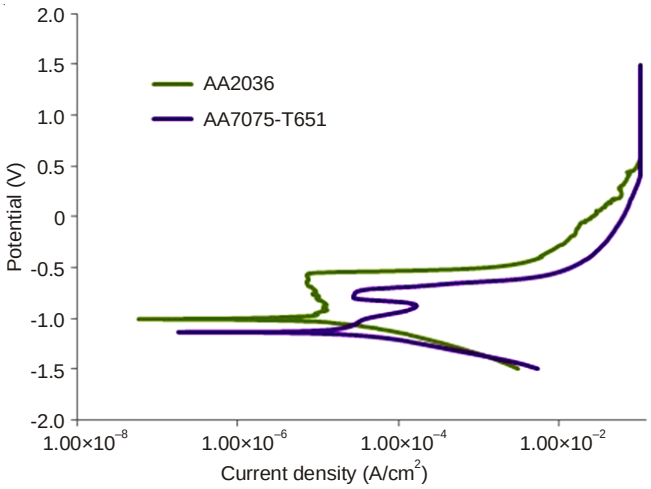

Fig. 6. Tafel polarization curve for substrates AA2036 and AA7075-T651 in 3.5 % wt NaCl

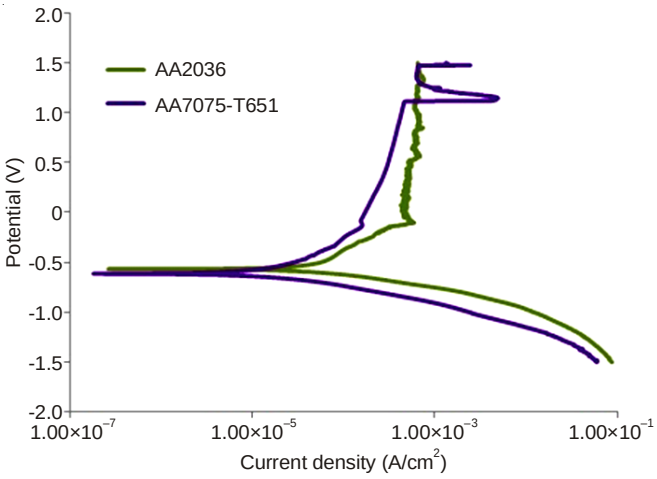

Fig. 7. Tafel polarization curve for substrates AA2036 and AA7075-T651 in 0.5 M H_2SO_4

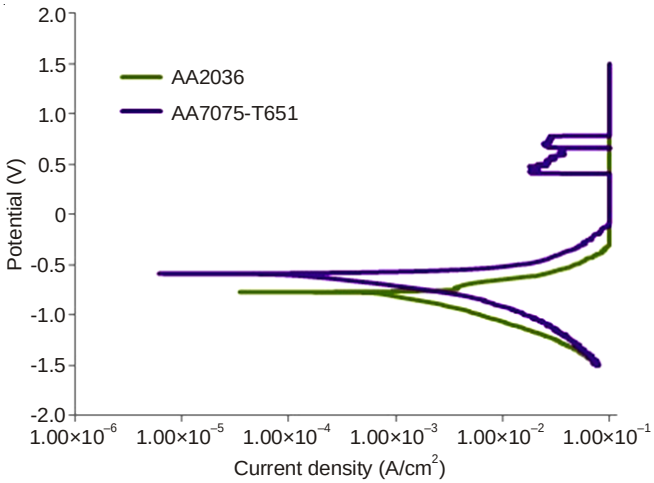

Fig. 8. Tafel polarization curve for substrates AA2036 and AA7075-T651 in 0.5 M HCl

is by far been protected against corrosion than AA7075-T651 alloy. These occurrences also correspond with the SEM results obtained with several pits formation.

Table-3 shows the data obtained from the polarization test, while Fig. 7 demonstrates the polarization curve for the

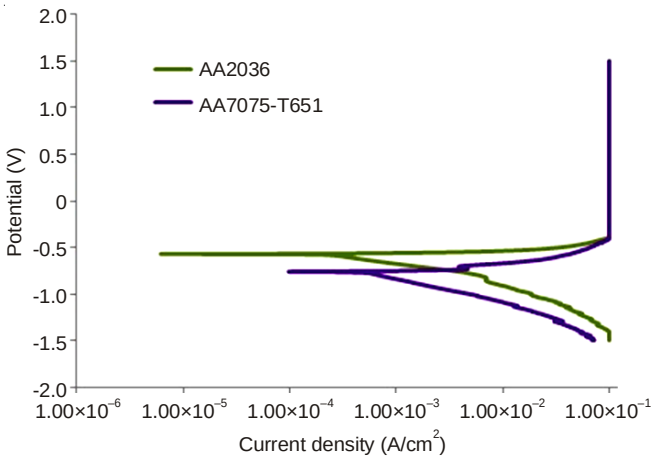

Fig. 9. Tafel polarization curve for substrates AA2036 and AA7075-T651 in 0.5 M H_2SO_4 + 3.5 % wt NaCl

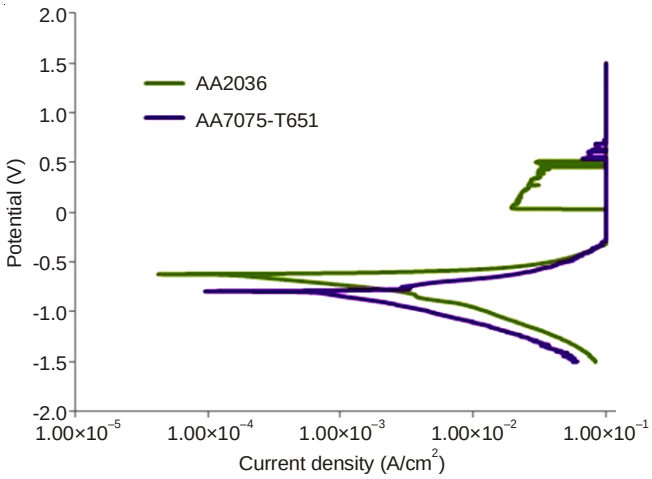

Fig. 10. Tafel polarization curve for substrates AA2036 and AA7075-T651 in 0.5 M HCl+ 3.5 % wt NaCl

substrates in 0.5 M H_2SO_4. According to electrochemical principle the samples with the lowest corrosion current has the lower corrosion rate in active stage and low linear polarization, this cause the passive film to break down thereby leading to localized corrosion.

In comparison, Tafel extrapolation in Fig. 8 showed that AA7075-T651 has the highest corrosion resistance followed than AA2036. The difference in their corrosion potential shows an improvement and better corrosion resistance which indicate a better material in such environment.

X-ray diffractometry (XRD) analysis of as-corroded aluminium alloys type AA2036 and AA7075-T651: Figs. 11-15 show the XRD patterns of different corroded samples in various environments. In the solution contain 3.5 wt % NaCl (Fig. 11), the XRD results of the corroded AA2036 and AA7075-T651 showed varying level of Al. Low XRD spectra of Al found on corroded AA7075-T651 surface compared to the corroded AA2036, suggested the influenced of corrosion attack on the sample. Perhaps shift in the inter-planar spacing (peak) was caused by stress cracking observed on their SEM images. Thus in agreement with the corrosion rate results (Fig. 1).

For the XRD spectrum of the corroded AA7xxx and AA2xxx samples, they are predominantly Al except for AA2xxx that has Fe in addition. However the spectra of

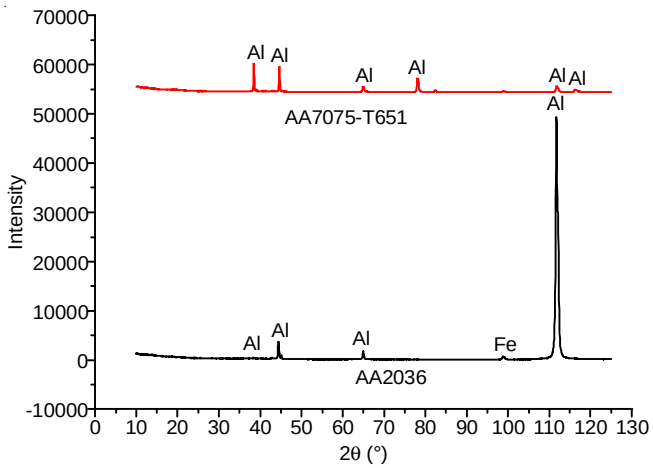

Fig. 11. XRD patterns of the corroded substrate samples in 3.5 % wt NaCl

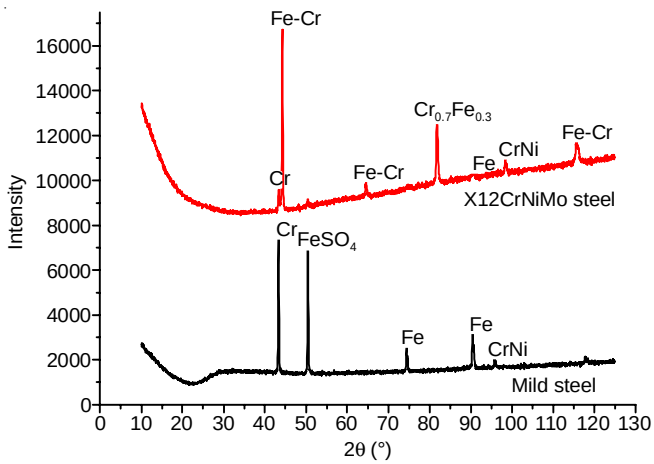

Fig. 12. XRD patterns of the corroded substrate samples in 0.5 M H_2SO_4 solution

AA7xxx was lower compared to AA2xxx, which has long peak at 2θ = 115°. Thus, suggested that AA7xxx was highly attacked in the solution (Figs. 1-5 and Table-3). Overall, it is of no doubt that Cl^- could not be found on both corroded AA2xxx and AA7xxx as a result of shifting in the peak or peak overlapping, as well as influence of corrosion.

For corroded AA7xxx and AA2xxx series, their XRD spectrum was predominantly Al (fcc), although the XRD peak of AA2xxx were lower than AA7xxx spectra. Nevertheless, no sulphate ion was found on their surface. Surprisingly, a low Fe peak observed to be overlapping at 2θ = 120° on AA7xxx. The reason could not be given and still unclear, perhaps could be due to the effect of corrosion on the elastic properties of the material. The XRD spectra of the samples immersed in 0.5 M H_2SO_4 + NaCl were showed in Fig. 13. The corroded AA2xxx and AA7xxx comprised of Al (FCC structure), while H_2SO_4 (H_2O) with an unknown peak found at 2θ = 82° detected on the corroded AA7xxx series. EDS revealed that some Fe, S, *etc.* is present on the corroded samples. Their omissions in the XRD spectra indicate that the amount may be too low to be detected. Thus, suggested that these minor elements might be underneath the corroded surfaces.

However, the presence of hydrated hydrogen sulphate revealed the rationale behind the worst performance of

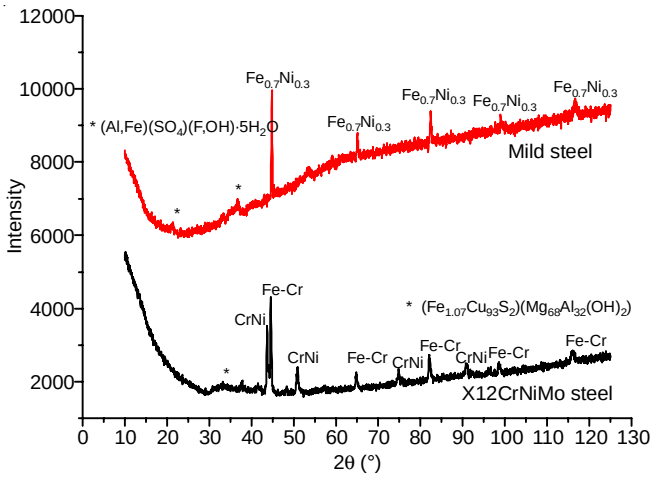

Fig. 13. XRD patterns of the corroded substrate samples in 0.5 M H_2SO_4 + NaCl solution

AA7xxx in the solution in comparison to others. Fig. 14 shows comparison of the corroded samples immersed in 0.5 M HCl + NaCl solution. The XRD pattern were similar for corroded AA7xxx and AA2xxx samples, indicating that the corroded surface comprised primarily Al. EDS scan revealed that Cl was present on the corroded samples. Its omission from the XRD spectra could be that the amount is too low to be detected.

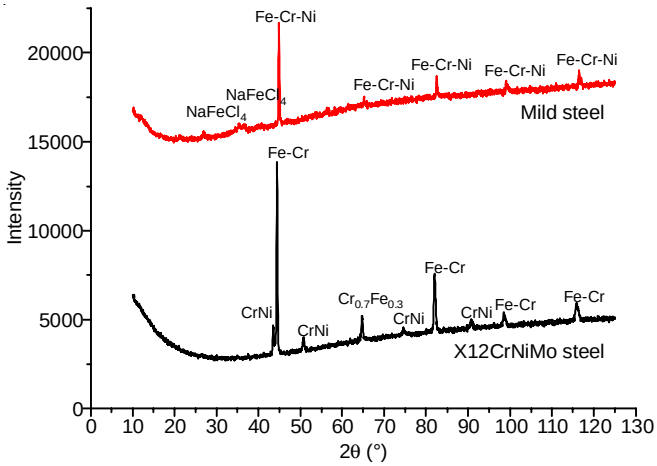

Fig. 14. XRD patterns of the corroded substrate samples in 0.5 M HCl+ NaCl solution

Fig. 15 shows the XRD patterns of the corroded samples immersed in HCl environment. Different phases were found on their corroded samples as expected, due to their physical properties, production, elemental composition and their percentage. All corroded sample in HCl had a highest peak at 50° to 40° (although the phases were different). The corroded AA7xxx revealed the presence of Al only, but their XRD peaks were extremely low as a result of corrosion effect. The presence of chlorine could not be found on the XRD as results of its amount. For corroded AA2xxx samples, the XRD spectrum was significantly different to AA7xxx sample. There were large Cu peak at 2θ = 44°, followed by Cu_2O peak at 2θ = 50°. In addition, three different phases were found: MgO0.6, MgO0.6, Cu and Al, which is expected. The formation of CuO could be due to affinity of Cu to oxygen caused by oxidation. This is in agreement with EDS results. Also, there was a higher

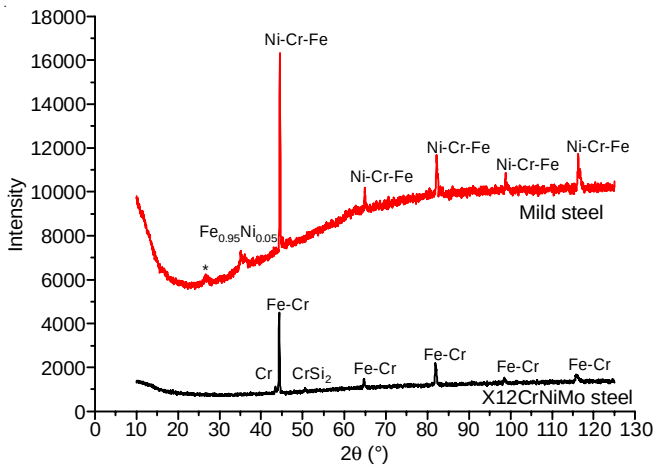

Fig. 15. XRD patterns of the corroded substrate samples in 0.5 M HCl solution

background between 2θ = 10-35°. This could be due to bleaching effect of chlorine on the corroded samples, as well as the effect of residual stress (strain).

Overall, the results showed that the degradation behaviour of AA2xxx is worst compare to AA7xxx in HCl solution. The emergence of complex compound of AA2xxx suggested the reason behind the worst performance.

Surface morphology of the corroded samples in acid-chloride/contaminated environments: The surface morphology of as-corroded AA2036 and AA7075-T651 has been assessed with scanning electron microscope in order to ascertain the degree of surface degradation and damage in various experimental conditions.

The micorgraphs reveals formation of widely salts precipitates and pits formation after 60 days of exposure of AA2036 in chloride media (Fig. 16). The grain boundary were not pronounced. The presence of chloride ion has a significant effect on the stability of the passive layer. EDS analysis revels that the film formed on AA2036 is composed of C, O, Cl, S, Mn.

Fig. 17 shows the SEM micrograph of AA7075T-651, the micorgraph reveals formation of salts precipitates in the pits after 60 days of exposure. The grain boundary were pronounced. EDS analysis reveals the chloride phases that were formed.

Figs. 18 and 19 show the SEM images of AA2023, AA7075-T651, respectively, morphological studies of the surfaces of the substrates in 0.5 M H_2SO_4 was carried out using SEM after immersion in the test environment for 60 days at room temperature. AA2023 and AA7075-T651 surfaces were characterized with pronounced pits formation. On the interfacial surface, the sulphuric ion gets entry by penetrating through the oxide film and attack the metal. The evidence of uniform and pitting corrosion was found in the alloy similar to Szklarska-Smialowka [11].

It can be seen in Figs. 22 and 23, those samples in the contaminated acid-chloride solution had the worst surface degradations including pits formation as a result of the chloride action on the reaction sites. This however correlates with the result obtained from the corrosion study for such samples in contaminated acid-chloride environments (Figs. 24 and 25).

Conclusion

The electrochemical behaviour of AA2xxx and AA7075-T651 in chloride, acidic and contaminated-acid-chloride media using weight loss and potentiodynamic polarization resulted in different corrosion behaviour. The corrosion rate of AA2036 in NaCl was found to be the lowest (0.058253 mm/yr) as compare with AA7075-T651 (0.14273 mm/yr) in the same environment and conditions. This means it has higher corrosion potential than AA7075-T651 indicating a 59 % improvement. The XRD spectra of the samples immersed in 0.5 M H_2SO_4 + NaCl were illustrated for corroded AA2xxx and AA7xxx which comprised of Al (FCC structure), while H_2SO_4 (H_2O) with an unknown peak found at 2θ = 82° detected on the corroded AA7xxx series. It was observed that the corrosion potentials of the aluminium alloys were drastically reduced when immersed in any of the contaminated environments. The alloys

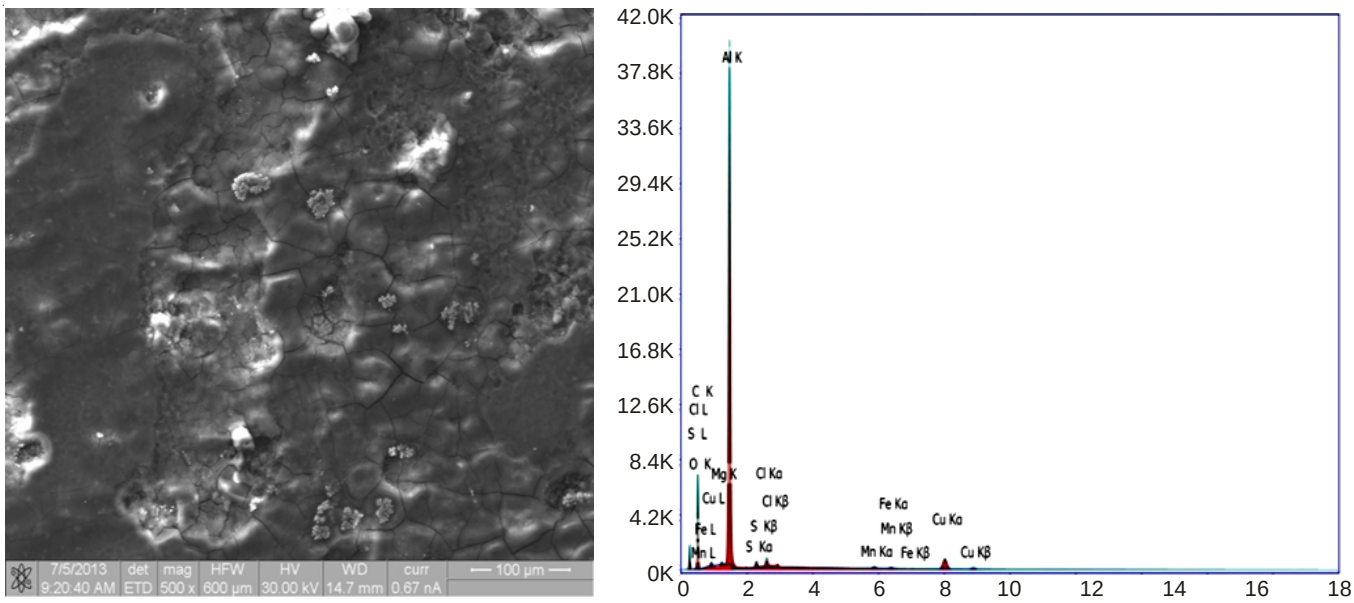

Fig. 16. SEM/EDS spectra of corroded AA2036 in 3.5 % wt NaCl solution

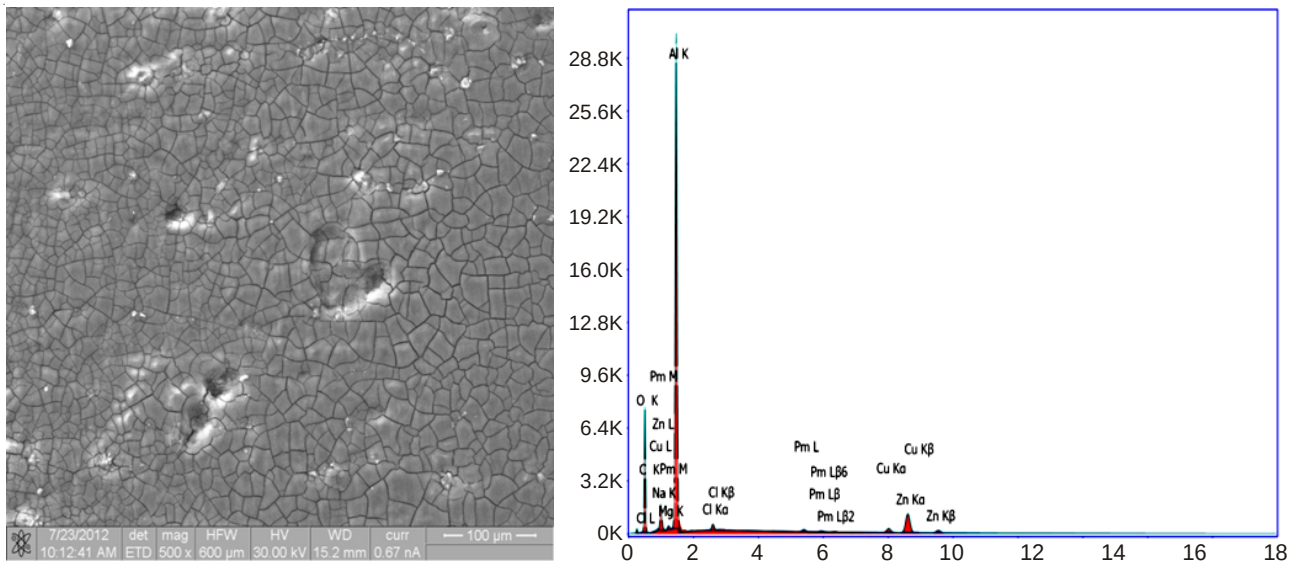

Fig. 17. SEM/EDS spectra of corroded AA7075-T651 in 3.5 % wt NaCl solution

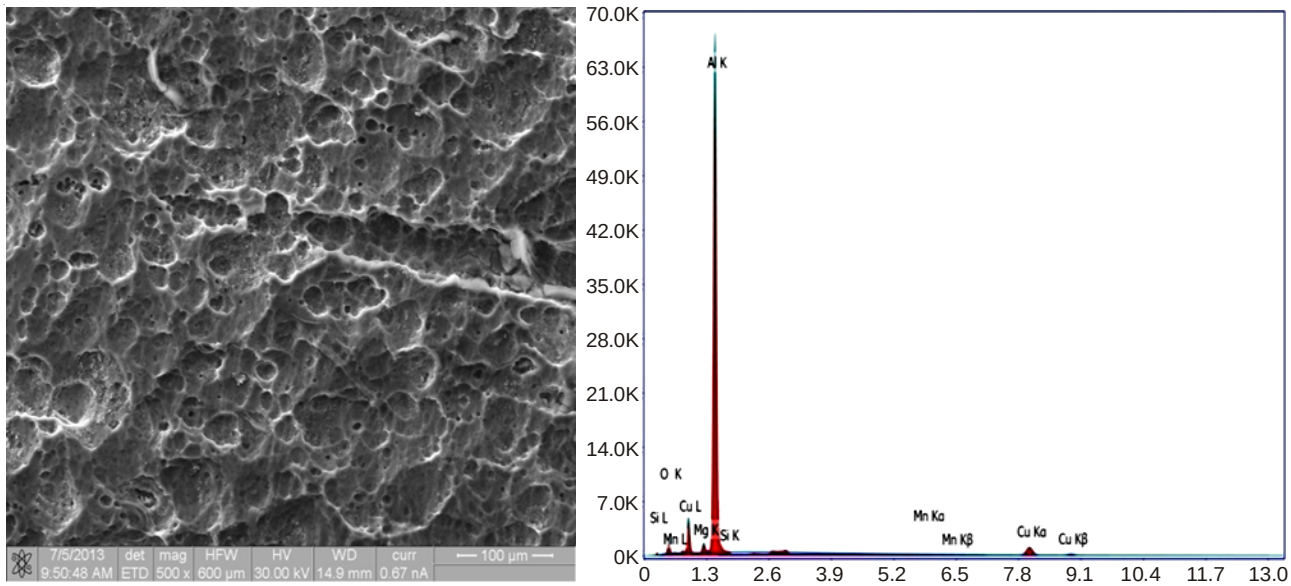

Fig. 18. SEM/EDS spectra of corroded AA2023 in 0.5 M H_2SO_4 solution

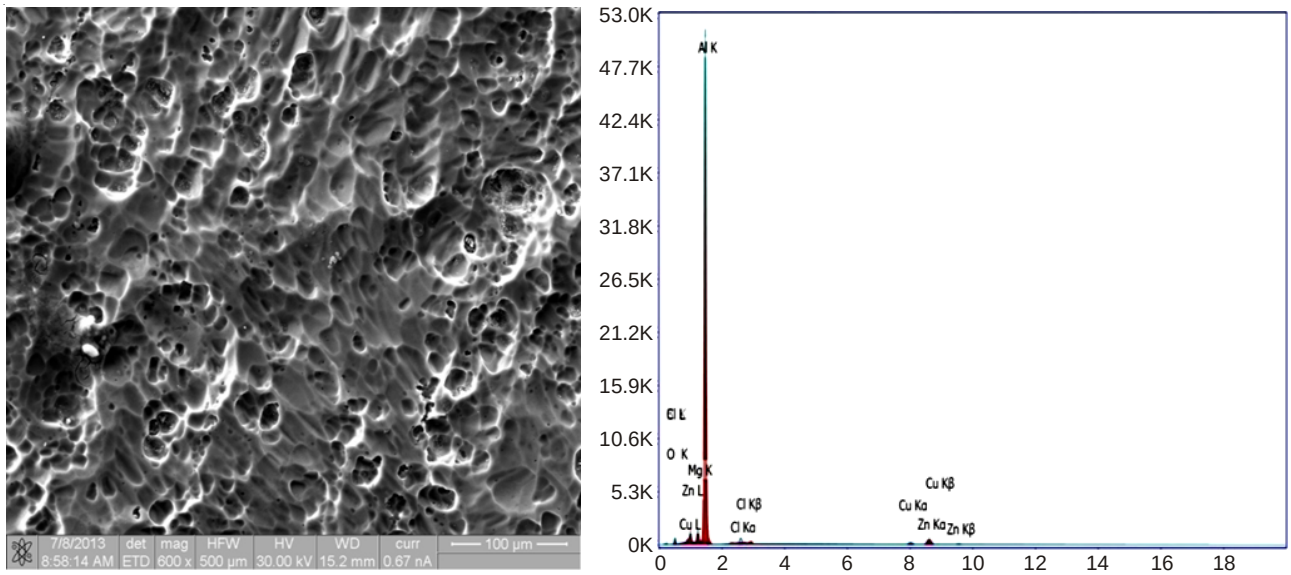

Fig. 19. SEM/EDS spectra of corroded AA7075-T651 in 0.5 M H_2SO_4 solution

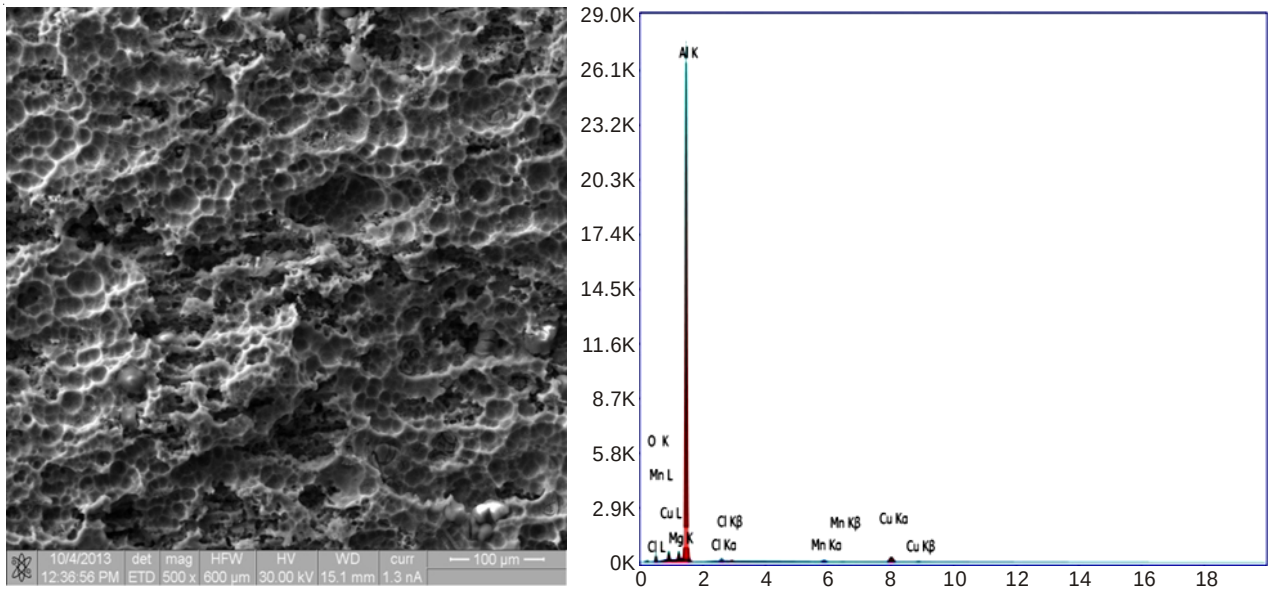

Fig. 20. SEM/EDS spectra of corroded AA2xxx in 0.5 M HCl solution

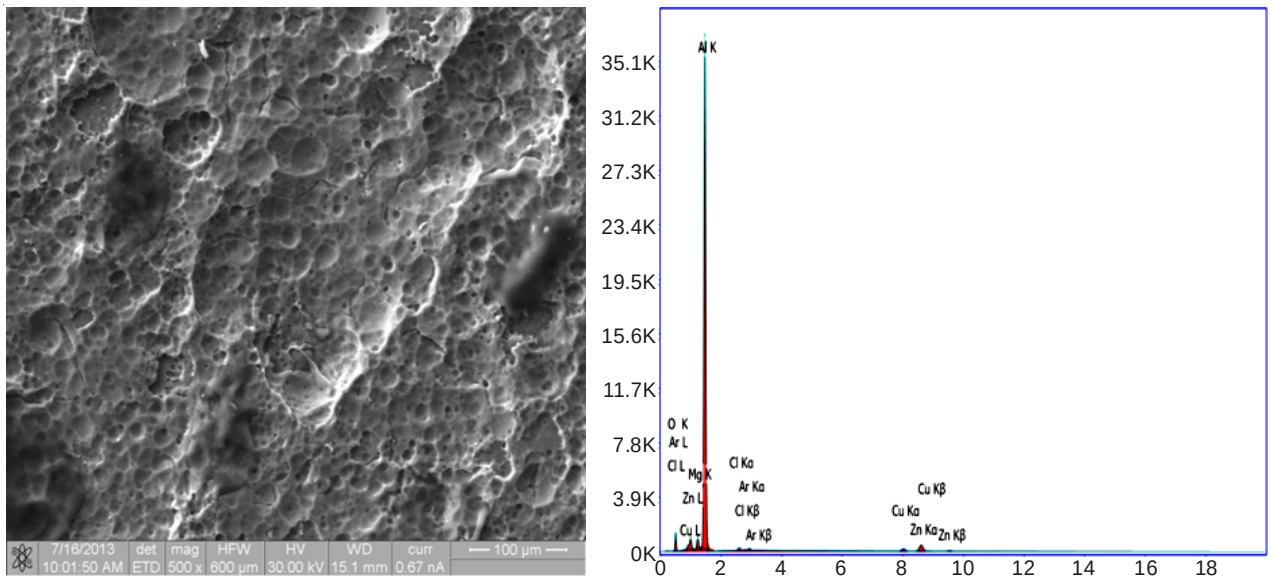

Fig. 21. SEM/EDS spectra of corroded AA7075-T651 in 0.5 M HCl solution

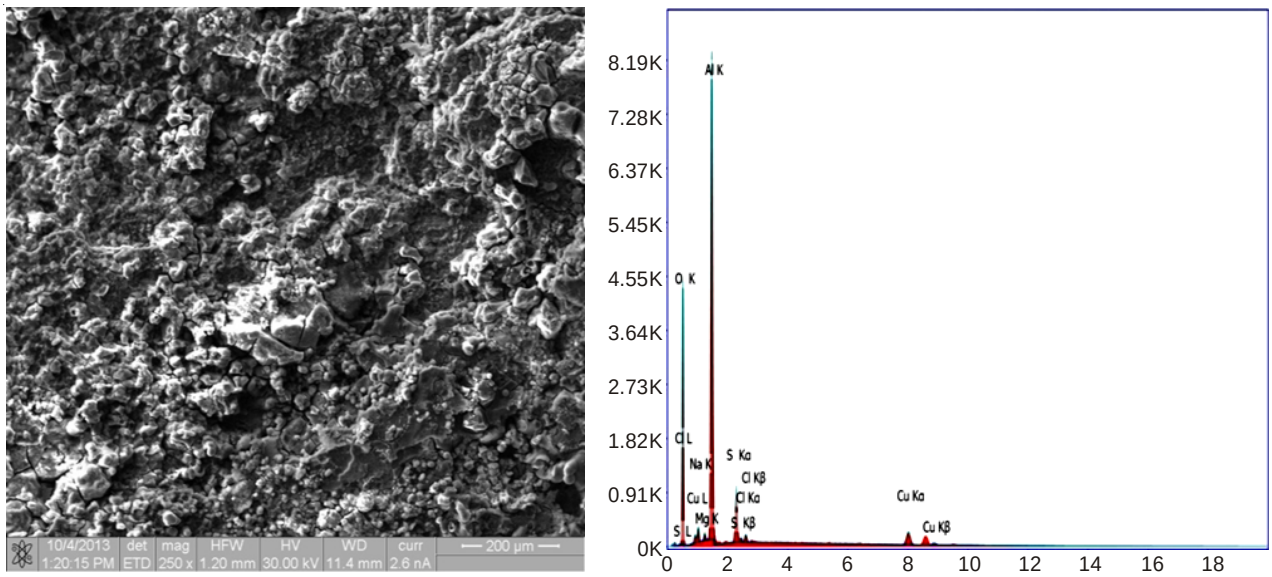

Fig. 22. SEM/EDS spectra of corroded AA2036 in 0.5 M H_2SO_4 + 3.5 NaCl solution

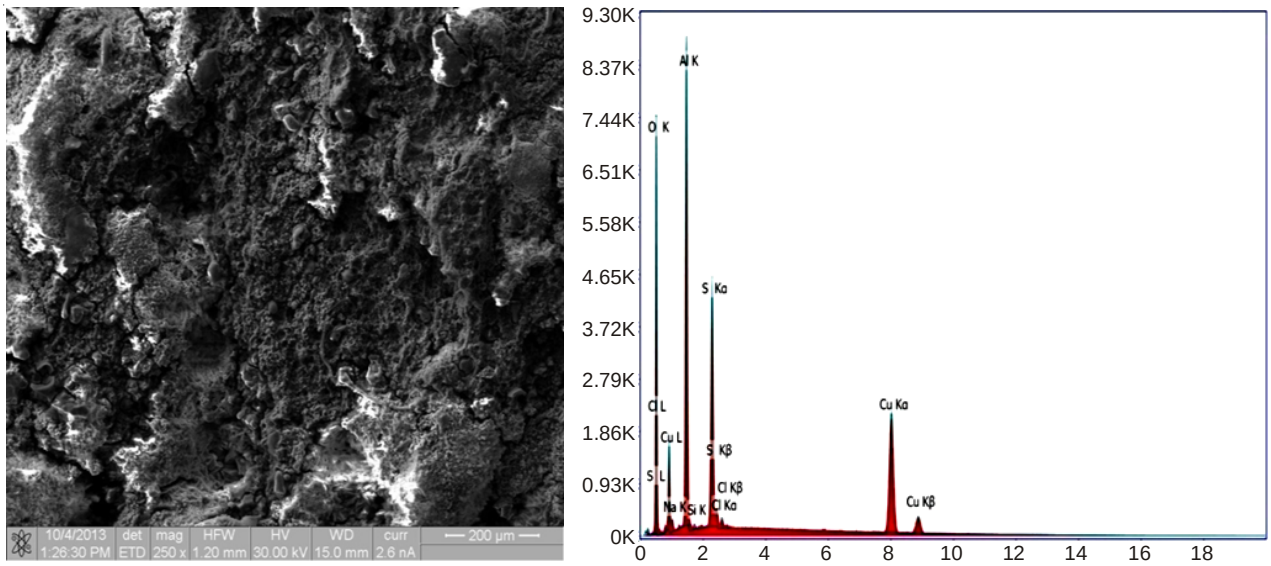

Fig. 23. SEM/EDS spectra of corroded AA7075-T651 in 0.5 M H_2SO_4 + 3.5 NaCl solution

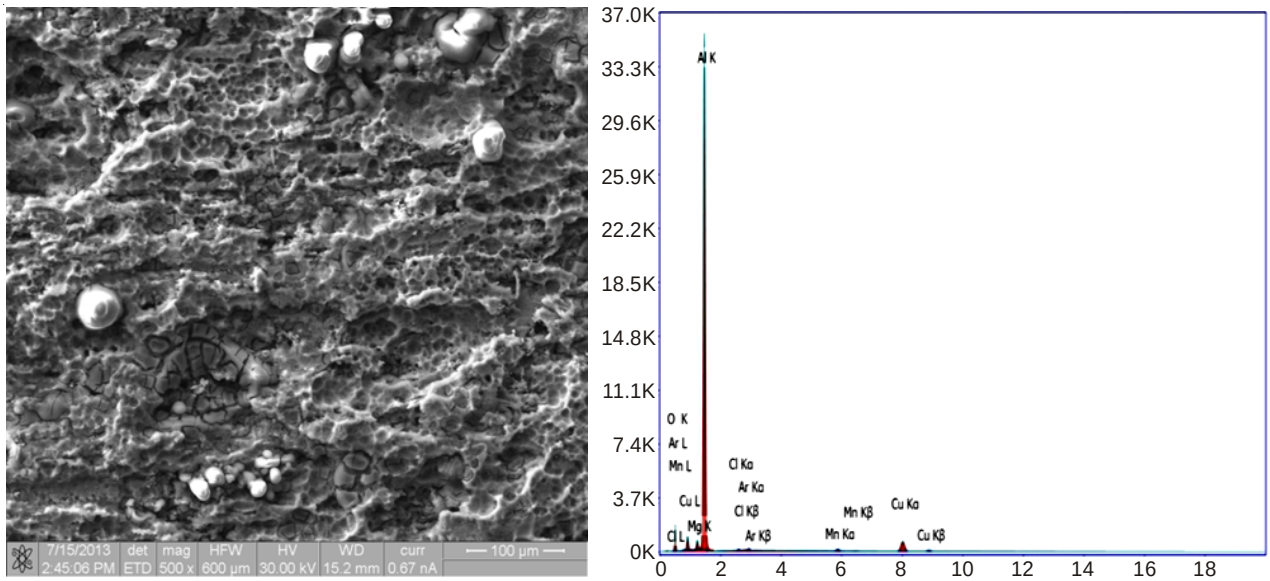

Fig. 24. SEM/EDS spectra of corroded AA2xxx in 0.5 M HCl + 3.5 % NaCl solution

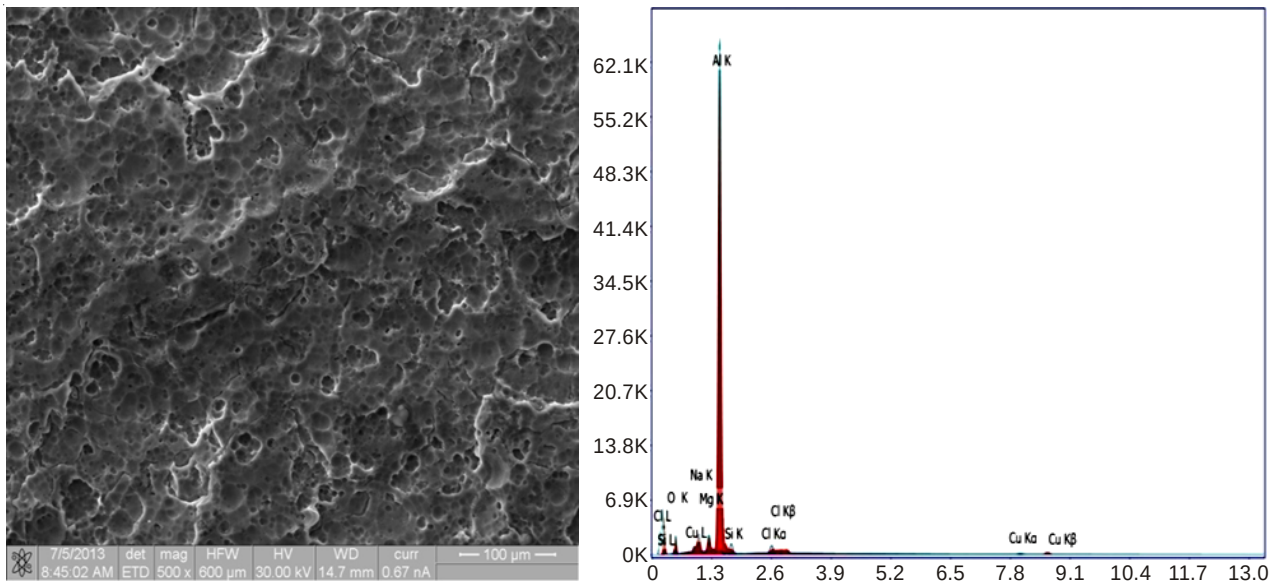

Fig. 25. SEM/EDS spectra of corroded AA7075-T651 in 0.5 M HCl + 3.5 % NaCl solution

when immersed in the contaminated acid-chloride solution had the worst surface degradations including pits formation as a result of the chloride action on the reaction sites. The evidence of pitting corrosion was characterized when the samples when used in various contaminated acid-chloride environments.

ACKNOWLEDGEMENTS

This material is based upon work supported financially by the National Research Foundation. The equipment support at Department of Chemical, Metallurgical and Materials Engineering, Pretoria, South Africa is highly appreciated.

REFERENCES

1. J. Hatch, Aluminium Properties and Physical Metallurgy, Metal Park (OH), ASM International, pp. 58-319 (1984).
2. E.A. Starke Jr. and J.T. Staley, *Prog. Aerosp. Sci.*, **32**, 131 (1996).
3. E.M. Sherif, *Int. J. Electrochem. Sci.*, **7**, 4235 (2012).
4. M.S. Kaiser and S. Dutta, *J. Mater. Sci. Chem. Eng.*, **2**, 52 (2014).
5. A. Aballe, M. Bethencourt, F.J. Botana, M.J. Cano and M. Marcos, *Corros. Sci.*, **43**, 1657 (2001).
6. K.M. Hijazi, A.M. Abdel-Gaber and G.O. Younes, *Int. J. Electrochem. Sci.*, **10**, 4366 (2015).
7. M. Abdulwahab, I.A. Madugu, S.A. Yaro, S.B. Hassan and A.P.I. Popoola, *Mater. Des.*, **32**, 1159 (2011).
8. B. Zaid, D. Saidi, A. Benzaid and S. Hadji, *Corros. Sci.*, **50**, 1841 (2008).
9. S. Tkaczyk and M. Kciuk, The Stress Corrosion Resistance Investigations of Aluminium AlMg5 Alloy, Proceedings of the 12th International Scientific Conference, Achievements in Mechanical and Materials Engineering, Gliwice-Zakopane, pp. 257-262 (2003).
10. J. David, Corrosion of Aluminium and Aluminium Alloys USA, ASM International, pp. 25-49 (1999).
11. Z. Szklarska-Smialowska, *Corros. Sci.*, **41**, 1743 (1999).